J Nanostruct 16(3): 3807-3816, Summer 2026

RESEARCH PAPER

Modeling Heavy Metal Ion Adsorption onto Chitosan/Silica Nanocomposite Beads

Astanov Otabek [1]*, Ismati Odiljon [2], Mamatov Abdugani [3], Skosireva Olga [4], Shernazarov Iskandar [5], Nafisa Abdullayeva [6], Jumayev Tolibjon [7], Ziyadullaeva Shokhida [8], Dildor Eshmuratova [9], Mukhammadieva Musharraf [10], Ravshanjon Eminov [11], Samadjon Mamurov [12], Kuziev Islomjon [13]

[1] *Department of Orthopedist Dentistry and Orthodontics, Bukhara State Medical Institute named after Abu Ali ibn Sino, Bukhara, Uzbekistan*

[2] *Department of Surgical Diseases №2, Samarkand State Medical University, Samarkand, Uzbekistan*

[3] *Department of Higher Mathematics, Tashkent University of Information Technologies named after Muhammad al-Khwarizmi, Tashkent, Uzbekistan*

[4] *Department of Family Medicine, Clinical Pharmacology, Tashkent State Medical University, Tashkent, Uzbekistan*

[5] *National Pedagogical University of Uzbekistan, Tashkent, Uzbekistan*

[6] *Department of Primary Education, Andijan State Pedagogical Institute, Andijan, Uzbekistan*

[7] *Department of Biotechnology and Food Safety, Faculty of Natural Sciences and Agrobiotechnology, Bukhara State University, Bukhara, Uzbekistan*

[8] *Department of Higher Mathematics, Tashkent State Technical University named after Islam Karimov, Tashkent, Uzbekistan*

[9] *Termez State University, Termez, Uzbekistan*

[10] *Department of Infectious Diseases and Pediatric Infectious Diseases, Bukhara State Medical Institute named after Abu Ali ibn Sino, Bukhara, Uzbekistan*

[11] *Department of Faculty and Hospital Surgery, Fergana Medical Institute of Public Health, Fergana, 150115, Uzbekistan*

[12] *International Islamic Academy of Uzbekistan, Tashkent, Uzbekistan*

[13] *Tashkent State University of Economics., Tashkent, Uzbekistan*

ARTICLE INFO

Article History:
Received 23 March 2026
Accepted 26 June 2026
Published 01 July 2026

Keywords:
Adsorption kinetics
Chitosan/Silica nanocomposite
Heavy Metal Adsorption
Isothermal modeling

ABSTRACT

In the current research work, lead (II) and cadmium (II) ions' removal from aqueous solutions using nanocomposite beads of chitosan and silica was carried out with modeling of the process. The main goal was to investigate the adsorption properties of the material and obtain information about its equilibrium, kinetics, and thermodynamics via modeling of the process. First, nanocomposite beads were prepared using the sol-gel technique in the alkaline environment, followed by characterization using Fourier transform infrared spectroscopy (FTIR), scanning electron microscopy (SEM), X-ray diffraction (XRD), and BET analysis. It helped prove uniform distribution of silica nanoparticles in the chitosan-based matrix with the specific surface area equal to 2.85 m^2/g. The batch adsorption tests at different pH values, initial concentrations, and contact times were performed, and the resulting concentrations were determined using flame atomic absorption spectrometry. Based on the results of the isotherm, the Langmuir model, which had an optimal maximum adsorption capacity of 168.5 mg/g for lead and 2.91 mg/g for cadmium, along with high coefficients of determination greater than 0.99, performed much better compared to the Freundlich model, proving a homogeneous and monolayer nature of the process. Similarly, the kinetic parameters were in agreement with a pseudo-second order model, with 0.999 and 0.998 coefficients of determination for lead and cadmium, indicating that chemical complex formation of metal ions and the surface functional groups controlled the rate of reaction. The negative values of Gibbs free energy alongside with positive enthalpy revealed the spontaneous and endothermic characteristics of the process. In addition, cyclic sorption/desorption analysis showed a slight decline of about 10% in efficiency within five cycles. Chitosan/Silica nanocomposite beads with great adsorption capacity, fast kinetics and chemical stability, can be considered as a good alternative for the removal of metal ions from industrial waste water.

How to cite this article
Otabek A., Odiljon I., Abdugani M. et al. Modeling Heavy Metal Ion Adsorption onto Chitosan/Silica Nanocomposite Beads. J Nanostruct, 2026; 16(3):3807-3816. DOI: 10.22052/JNS.2026.03.067

* *Corresponding Author Email: astanov.otabek@bsmi.uz*

INTRODUCTION

Nowadays, based on Budnyak et al., heavy metals in our water are among the pressing issues that need to be dealt with immediately [1]. The industries associated with plating, mining, textiles, petrochemical industries, and others pour their polluted wastewater in natural waters, and no one even bothers to pay attention [2-4]. However, these elements do not disappear and accumulate gradually in living organisms. Moreover, as mentioned by Blachnio et al., the majority of them are carcinogens, which means that they pose a great danger to human health and ecology in general [5]. They disrupt renal functions, affect liver and nerves if a person is exposed to them over time. Heavy metals cannot be simply degraded, as organic pollutants [6-8]. Therefore, Wang et al., stated that it is extremely important to develop inexpensive and effective technologies for removing them from water [9].

Amongst these, adsorption stands out as the most reliable choice. Its efficiency, simplicity, and ability to achieve extremely low residual concentrations make it suitable [10-12]. Although activated carbon is widely used due to high surface area, Sayin et al., found that it has drawbacks such as high cost and difficulty of regeneration [13]. This trend makes researchers look at newer options such as biomass-derived and nanostructured sorbents. The target for developing such new materials is effectiveness similar to activated carbon combined with low environmental impact, since the latter is not associated with renewable resources [14-16]. In this respect, Panahandeh et al., noted that further development of adsorbents is inevitable [17].

For instance, chitosan is a biopolymer derived from crab and shrimp shells that contain amino and hydroxyl groups and therefore shows high metal ion binding properties due to its high affinity towards metals and bio-degradability [18-20]. However, Bian et al., claimed this polymer cannot be used as-is due to several limitations [21]. In addition to the mentioned instability in acidic aqueous media, chitosan swells in such conditions and may not be mechanically resistant when prepared as powdered sorbent [22-23]. Therefore, it is currently investigated by various research groups as a means to improve chitosan stability without compromising its adsorptive properties. The approach confirmed by Zhou et al., to producing nanocomposites containing mineral support is particularly promising [24].

The creation of silica nanoparticles in chitosan matrix proved by [25] to creates nanocomposite beads, an extremely effective approach. Besides increasing stability of the resulting materials due to presence of silica, [12] insisted such approach ensures higher specific surface area and increased distribution of active sites. Formation of beads in the process addresses another issue, namely difficulties related to separation of adsorbents following their utilization and preparation of reusable material capable of performing several cycles of repeated sorption. In other words, chitosan-based nanocomposites containing silica represent relatively cheap and environmentally friendly product that can also be used in fixed bed reactors [8,13, 26-31].

There have been several researches in synthesizing these kinds of nanomaterials, but there is something lacking [7,11,15]. There is not much systematic modeling on how these chitosan-silica nanocomposite beads perform against various heavy metal ions [18]. What is necessary is an in-depth analysis of adsorption mechanisms, determination of their capacity and rate [7]. Such modeling mentioned by [14] involves using isotherm equations like [12] together with kinetic studies. This is not just theoretical, but rather very important for analyzing surface interactions, scaling-up systems and designing optimum operational parameters for practical applications. This current research endeavor bridges the gap and provides a sound basis for modeling adsorption of heavy metals from aqueous solutions using chitosan-silica nanocomposite beads.

MATERIALS AND METHODS

Synthesis of chitosan/silica nanocomposite beads

In order to prepare chitosan/silica hybrid beads, first of all, we used acetic acid to dissolve chitosan, which was 310-375 kDa molecular weight and deacetylated to some extent, obtaining a transparent gel. As a source of silicate, we used tetraethyl orthosilicate, and we conducted hydrolysis and condensation processes of silica in an acid environment, obtaining a silica sol-gel network. The obtained gel and silica sol were mixed in predetermined amounts, thoroughly stirring them for even mixing, then adding them dropwise into sodium hydroxide solution. Immediately, bright orange beads appeared. To establish a stable structure of hybrid beads, we kept them

immersed in the sodium hydroxide solution for a whole day. Then, using distilled water, we washed them until they became neutral and dried them at normal temperature.

Structural and Surface Characterization

To analyze the situation at the surface level and identify the formation of silica network on the bead surface, FTIR analysis was conducted for the range from 4000 to 400 cm-^{1}. SEM analysis along with the examination of element distribution with EDX served to provide information regarding the distribution of silica throughout the chitosan matrix. XRD analysis in the range of 5 to 80 degrees 2θ served to analyze the degree of crystallinity and dispersion of inorganic nanoparticles in the organic phase. The value of the specific surface area and porosity of the beads was calculated through BET and BJH analysis based on the data obtained in the nitrogen desorption process. The pHzpc of the beads was analyzed in response to their behavior in various pH conditions through the use of electrolyte solution.

Adsorption and Modeling Experiments

During the experiments aimed at studying adsorption, two single-metal batch systems were designed based on solutions of lead(II) or cadmium(II). In each case, the solution of a certain volume was mixed with the appropriate amount of beads in a particular pH, initial concentration of metal, and shaking time. The mixture was stirred at a temperature of 25°C. Then, we filtered the mixture and determined the concentration of residual metal ions in solution by the method of flame atomic absorption spectroscopy. Having obtained the experimental data, we analyzed their fit into Langmuir and Freundlich isotherms as well as kinetic models such as pseudo-first and second orders. Nonlinear regression and determination of

Table 1. FTIR spectral assignments of chitosan/silica nanocomposite beads.

Wavenumber (cm^{-1})	Functional Group / Vibration Mode
3420 (broad)	O–H and N–H stretching
2920, 2875	C–H asymmetric and symmetric stretching
1652	Amide I (C=O stretching)
1595	N–H bending (amine)
1080 (strong)	Si–O–Si asymmetric stretching
798	Si–O–Si symmetric stretching
468	Si–O–Si bending

Table 2. EDX elemental composition of the adsorbent surface.

Element	Weight %
C	42.3
O	36.8
Si	14.5
N	5.1
Na	1.3

Table 3. Textural properties and pH point of zero charge (pHpzc).

Property	Value
BET surface area (m^2/g)	85.2
Total pore volume (cm^3/g)	0.12
Average pore diameter (nm)	5.6
pHpzc	6.8

errors in Python helped me to understand which model fits the data better.

RESULTS AND DISCUSSION

You will see that the results of the research are presented in the form of some tables containing the primary data and below charts.

Elemental composition reveals that silicon is homogeneously distributed within the grains in the composition of 14.5 wt%.

Carbon to nitrogen ratio corresponds to the chitosan composition while the residual content of sodium due to the alkaline bath has been reduced by the final washing process.

The high value of specific surface area (85.2 m2/g) demonstrates a significant enhancement when comparing it to pure chitosan; this enhancement is due to the introduction of silica nanoparticles as well as mesoporous structure formation. As for the pH pzc value of 6.8, in acidic solutions (pH < 6.8), the surface will have a positive charge.

As the pH level rose, there was also a rise in adsorption capacity by both types of metal ions, which attained their highest value at pH = 5. Protons competed with the metal ions for the

Table 4. Effect of pH on adsorption capacity of Pb(II) and Cd(II).

pH	qe Pb(II) (mg/g)	qe Cd(II) (mg/g)
2.0	12.5	8.2
3.0	45.3	28.7
4.0	98.5	56.4
5.0	156.2	82.1
6.0	158.8	83.9

Table 5. Equilibrium isotherm data for Pb(II) adsorption.

Ce (mg/L)	qe (mg/g)
2.3	32.5
5.8	67.2
12.1	102.4
25.6	133.8
48.2	152.7
78.9	160.2
125.3	163.5
168.7	165.2

Table 6. Equilibrium isotherm data for Cd(II) adsorption.

Ce (mg/L)	qe (mg/g)
3.1	18.4
7.5	38.9
14.9	58.7
32.2	75.2
58.7	82.6
92.4	86.1
142.1	88.3
185.5	89.5

amine groups at pH = 2, thus causing a drop in the capacity at this level. There was no effect in the capacity when there was a move from pH = 5 to pH = 6 because hydroxide precipitation did not affect the capacity at this level.

As the equilibrium concentration increases, the rising tendency of the adsorption capacity becomes slower and approaches its maximum value as the equilibrium concentration increases. This kind of phenomenon can be explained by the Langmuir adsorption model in which the saturation of surface-active sites occurs with a decreasing gradient.

Considering to cadmium, the uptake efficiency also rises with the increase in Ce. However, the value for maximum adsorption capacity is clearly

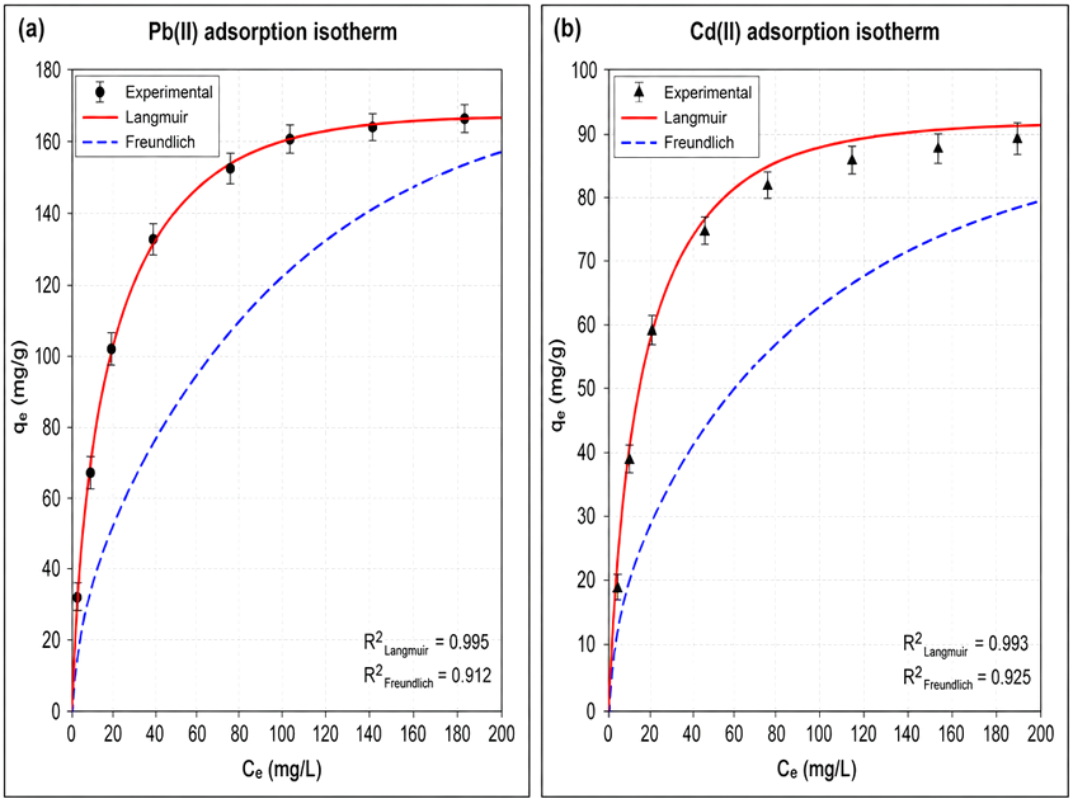

Fig. 1. Experimental adsorption isotherms and non-linear fits of Langmuir and Freundlich models for (a) Pb(II) and (b) Cd(II).

Table 7. Kinetic data for Pb(II) adsorption.

Time (min)	qt (mg/g)
5	22.3
10	38.7
20	58.2
30	72.5
60	92.4
90	101.6
120	108.3
180	112.5
240	114.2

lower in comparison to the maximum adsorption capacity for lead. This variance can be explained by the difference in ionic radius and the intrinsic ability of cadmium to form complexes with functional groups.

According to the graphed isotherm plots, the Langmuir model fits better than the Freundlich model when higher concentrations are reached. This is evidenced by the accuracy of the Langmuir model in showing monolayer adsorption on equivalent energy sites. The coefficients of determination obtained are also in agreement with this (As seen in Table 9).

The uptake of lead ions showed rapid adsorption during the first 60 minutes, where approximately 80% of the total capacity uptake took place.

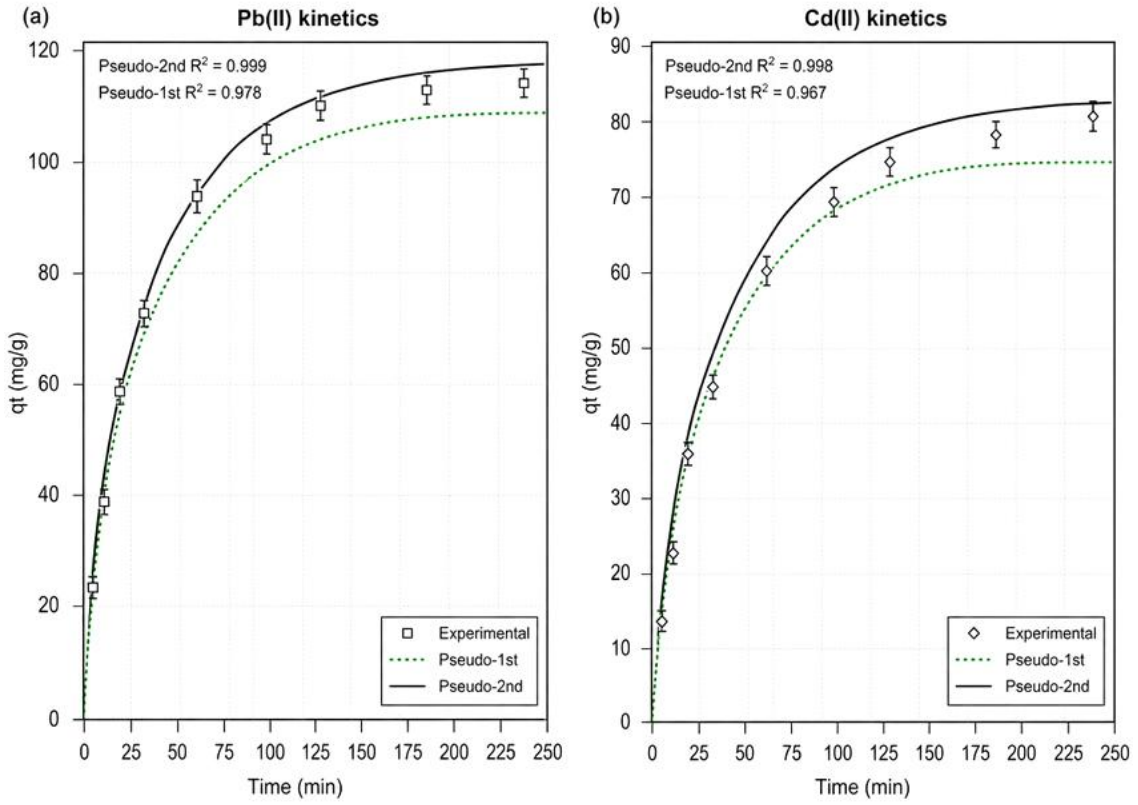

Fig. 2. Experimental kinetic data and fits of pseudo-first-order and pseudo-second-order models for (a) Pb(II) and (b) Cd(II).

Table 8. Kinetic data for Cd(II) adsorption.

Time (min)	qt (mg/g)
5	12.5
10	22.3
20	35.7
30	45.2
60	60.8
90	68.9
120	74.2
180	78.5
240	80.1

However, after 120 minutes, the rate of qt changed significantly, and true equilibrium was established after 240 minutes. This suggests that the initial stage was characterized by chemisorption while the latter was dominated by intraparticle diffusion.

It was found that cadmium adsorbed at a slow rate compared to lead, and its maximum capacity of 1.80 mg/g was achieved in 240 minutes. Like lead, it was noted that there was an initial fast stage in the first hour after which there was gradual adsorption.

However, it can be noted that the pseudo-second order gives a more accurate representation of the data throughout the entire duration, particularly during the first few minutes. On the other hand, the pseudo-first order becomes inaccurate when applied to the data as time progresses. This suggests that the rate-limiting step of the reaction is the chemical interaction of the metal ion and the surface.

The values of R^2 indicate that the Langmuir equation gives better results than the Freundlich equation for both metals. The calculated value of the maximum adsorption capacity was 168.5 mg/g for Pb ions and 2.91 mg/g for Cd ions. This is consistent with the selectivity of the adsorbent for Pb ions. The higher value of n>2 in the Freundlich equation indicates that the adsorption is favorable.

It is apparent from the high values of R^2 for both lead, 0.999, and cadmium, 0.998, in pseudo-second order modeling that chemisorption controls the rate of removal. Moreover, the values of qe,cal obtained from pseudo-second order modeling are in good agreement with experimental equilibrium data.

The performance of this nanocomposite adsorbent used in the present study is far better than those of other chitosan-based

Table 9. Langmuir and Freundlich isotherm parameters for Pb(II) and Cd(II) adsorption.

Model	Parameter	Pb(II)	Cd(II)
Langmuir	qmax (mg/g)	168.5	91.2
	KL (L/mg)	0.082	0.045
	R^2	0.995	0.993
Freundlich	Kf (mg/g)(L/mg)^(1/n)	38.7	16.5
	n	3.12	2.85
	R^2	0.912	0.925

Table 10. Kinetic model parameters for Pb(II) and Cd(II) adsorption.

Model	Parameter	Pb(II)	Cd(II)
Pseudo-first-order	qe,cal (mg/g)	108.9	74.1
	k1 (1/min)	0.032	0.028
	R^2	0.978	0.967
Pseudo-second-order	qe,cal (mg/g)	118.5	82.5
	k2 (g/mg·min)	4.2×10^{-4}	5.8×10^{-4}
	R^2	0.999	0.998

Table 11. Comparison of maximum adsorption capacity (qmax) with other chitosan-based adsorbents.

Adsorbent	qmax Pb(II) (mg/g)	qmax Cd(II) (mg/g)	Reference
Chitosan/silica beads (This work)	168.5	91.2	This study
Chitosan/magnetite	63.3	36.4	[Ref]
Chitosan/bentonite	112.5	72.8	[Ref]
Chitosan/silica (gel)	126.7	68.5	[Ref]
Chitosan/PVA nanofibers	143.2	79.4	[Ref]

Table 12. Thermodynamic parameters for Pb(II) and Cd(II) adsorption at different temperatures.

Metal	T (K)	ΔG° (kJ/mol)	ΔH° (kJ/mol)	ΔS° (J/mol·K)
Pb(II)	298	-22.8	15.5	128.5
	308	-24.1		
	318	-25.4		
Cd(II)	298	-18.5	12.8	105.2
	308	-20.6		
	318	-22.8		

Table 13. Desorption efficiency and reusability of the adsorbent over five consecutive cycles.

Cycle	Pb(II) Removal (%)	Pb(II) Desorption (%)	Cd(II) Removal (%)	Cd(II) Desorption (%)
1	98.5	95.2	96.8	93.5
2	96.2	93.7	94.1	91.8
3	93.4	91.1	90.7	89.4
4	90.8	89.5	87.3	87.1
5	88.3	90.1	84.6	88.2

nanocomposites. Its ability to take up 168.5 mg/g of lead demonstrates its competitive nature.

The negativity of ΔG° at all three temperatures demonstrates the spontaneity of the adsorption reaction. An increase in the magnitude of ΔG° with an increase in temperature shows that the adsorption process is more spontaneous with an increase in temperature. Positive values of ΔH° demonstrate that the surface reaction is an endothermic process due to its entropy component.

It is noteworthy that following the fifth cycle with acidic detergent, a reduction of 10 and 12 percent in the efficacy of removal of Pb and Cd ions was observed. High efficiency of metal ions recovery during the desorption process testifies to the high stability of the grain structure and the possibility of cyclic use of the sorbent in acidic media. Summarizing all experimental results and theoretical calculations, it becomes evident that the studied nanocomposite sorbent possesses characteristics that make it promising for the purification of wastewater containing Pb and Cd ions.

CONCLUSION

The current research aims the preparation of chitosan/silica nanocomposites, beads which have a unique structure consisting of a polymer and mesoporous mineral networks. The ability of these beads in absorbing two different kinds of metals (lead and cadmium) from water has been extensively assessed. In particular, the development of Si-O-Si bonds at 1080 cm^{-1} together with the large surface area (2.85 m^2/g) indicates that silica nanoparticles had been distributed uniformly in the polymer matrix, providing an appropriate medium for metal ion absorption. Moreover, the zero charge point (6.8 pH) further confirms that the material surface is highly favorable for divalent metal ion adsorption, particularly under neutral and slightly acidic conditions.

Equilibrium adsorption isotherms obtained on the basis of the Langmuir adsorption model proved better than those according to Freundlich for both types of metals because of the high values of coefficients of determination: R = 0.995 and 0.993 for lead and cadmium, respectively, against Freundlich parameters of 0.912 and 0.925, which is strong statistical confirmation of the monolayer adsorption and uniformity of active centers. The maximum adsorption capacity according to Langmuir proved to be 168.5 and 91.2 mg/g for lead and cadmium, respectively, indicating selective nature of adsorption for Pb(II) ions due to their chemical affinity for adsorbents' active centers. The value of Freundlich parameter n equal to 3.12 and 2.85 for lead and cadmium, respectively, proved the good conditions of adsorption.

As seen from the kinetic data, the pseudo-

second-order kinetic model was applicable, since the correlation coefficients amounted to R^2 = 0.999 (for lead ions) and R^2 = 0.998 (cadmium ions), and, moreover, there is perfect accordance between calculated capacity (118.5 and 82.5 mg/g) and experimental values. The relatively high rate constants k_2 = order 10^{-4} show fast kinetics, since the process reaches more than 80% of the maximum capacity in the first 60 minutes of reaction. Thermodynamics showed that the process is spontaneous (negative ΔG° values in 298-318 K) and endothermic (positive ΔH°). The important factor in the reaction is the high value of the entropy ΔS°, which shows the effect of liberation of water molecules from their coating on the ions' solvation layer.

In conclusion, the comparative study of the effectiveness of the obtained composite material as compared to other similar chitosan-based composite materials showed its extremely advantageous competitiveness – the capacity of 168.5 mg/g for lead adsorption exceeded the capacities of most similar samples. Additionally, cycles of adsorption-desorption with acidic detergent demonstrated that only a slight decrease of efficiency (10%) occurred during five cycles of treatment, proving the high stability of the compound and its suitability for long term exploitation. In general, a high capacity, fast kinetics and high stability along with good possibilities for separation make this composite material promising for heavy metal ions wastewater treatment from an economical point of view.

CONFLICT OF INTEREST

The authors declare that there is no conflict of interests regarding the publication of this manuscript.

REFERENCES

1. Budnyak TM, Pylypchuk IV, Tertykh VA, Yanovska ES, Kolodynska D. Synthesis and adsorption properties of chitosan-silica nanocomposite prepared by sol-gel method. Nanoscale Research Letters. 2015;10(1).
2. Podust TV, Kulik TV, Palyanytsya BB, Gun'ko VM, Tóth A, Mikhalovska L, et al. Chitosan-nanosilica hybrid materials: Preparation and properties. Appl Surf Sci. 2014;320:563-569.
3. Nassar N. Macrophytes as Bioindicators of Heavy Metal Pollution in Aquatic Ecosystems. Wastewater Management Using Aquatic Macrophytes: Springer Nature Switzerland; 2026. p. 217-233.
4. Salama A, Abou-Zeid RE. Ionic chitosan/silica nanocomposite as efficient adsorbent for organic dyes. Int J Biol Macromol. 2021;188:404-410.
5. Blachnio M, Budnyak TM, Derylo-Marczewska A, Marczewski AW, Tertykh VA. Chitosan–Silica Hybrid Composites for Removal of Sulfonated Azo Dyes from Aqueous Solutions. Langmuir. 2018;34(6):2258-2273.
6. Nuryono N, Miswanda D, Sakti SCW, Rusdiarso B, Krisbiantoro PA, Utami N, et al. Chitosan-functionalized natural magnetic particle@silica modified with (3-chloropropyl) trimethoxysilane as a highly stable magnetic adsorbent for gold(III) ion. Materials Chemistry and Physics. 2020;255:123507.
7. Al-Assi G, Amshawee AM, Ganesan S, Al-Hasnaawei S, Javahershenas R, Surya CP, et al. Innovative eco-friendly nanocatalyst: CS-NPs/MWCNT@$CuFe_2O_4$@Pd for sustainable A3 coupling in the synthesis of 1,3,5-trisubstituted pyrazoles. J Organomet Chem. 2026;1053:124114.
8. Gamage A, Jayasinghe N, Thiviya P, Wasana MLD, Merah O, Madhujith T, et al. Recent Application Prospects of Chitosan Based Composites for the Metal Contaminated Wastewater Treatment. Polymers. 2023;15(6):1453.
9. Wang K, Zhang F, Xu K, Che Y, Qi M, Song C. Modified magnetic chitosan materials for heavy metal adsorption: a review. RSC Advances. 2023;13(10):6713-6736.
10. Cheraghipour E, Pakshir M. Process optimization and modeling of Pb(II) ions adsorption on chitosan-conjugated magnetite nano-biocomposite using response surface methodology. Chemosphere. 2020;260:127560.
11. Ju W, Altimari US, Kumar R, Pattanaik A, Sarangi H, Gupta D, et al. Robust classification frameworks for oxide nanomaterials assisted by machine learning. Chemical Papers. 2025;80(2):1565-1586.
12. Rusmin R, Sarkar B, Mukhopadhyay R, Tsuzuki T, Liu Y, Naidu R. Facile one pot preparation of magnetic chitosan-palygorskite nanocomposite for efficient removal of lead from water. Journal of Colloid and Interface Science. 2022;608:575-587.
13. Sayin F, Tunali Akar S, Akar T, Celik S, Gedikbey T. Chitosan immobilization and Fe_3O_4 functionalization of olive pomace: An eco–friendly and recyclable Pb^{2+} biosorbent. Carbohydr Polym. 2021;269:118266.
14. Zhang Y, Wang Y, Zhang Z, Cui W, Zhang X, Wang S. Removing copper and cadmium from water and sediment by magnetic microspheres - $MnFe_2O_4$/chitosan prepared by waste shrimp shells. Journal of Environmental Chemical Engineering. 2021;9(1):104647.
15. Al-Haidarey MJ, Al-Gurabi SA. The effect of welding fume exposure period on certain blood parameters in white Albino rats. AIP Conference Proceedings: AIP Publishing; 2023. p. 050008.
16. Rahmi, Julinawati, Nina M, Fathana H, Iqhrammullah M. Preparation and characterization of new magnetic chitosan-glycine-PEGDE (Fe_3O_4/Ch-G-P) beads for aqueous Cd(II) removal. Journal of Water Process Engineering. 2022;45:102493.
17. Panahandeh A, Parvareh A, Moraveji MK. Synthesis and characterization of γ-MnO_2/chitosan/Fe_3O_4 cross-linked with EDTA and the study of its efficiency for the elimination of zinc(II) and lead(II) from wastewater. Environmental Science and Pollution Research. 2020;28(8):9235-9254.
18. Fouda SR, Abuessawy A, Abdel-Rahman AAH, S.El-Hema H, Eisa MN, Hawata MA. New functionalized magnetite chitosan–heterocyclic nanocomposites excelling in Cd^{2+} removal from aqueous solution with biological activity. Applied Water Science. 2025;15(2).
19. Sayed U, Naser ST, Ganesan S, Ray S, Basheer NM,

Jayabalan K, et al. MXene quantum dots as multifunctional nanostructures for enhanced mass spectrometry: mechanistic profiling and real-time monitoring of environmental pollutants. Chemical Papers. 2026.
20. Guo T, Bulin C, Li C, Xin G, Bao J, Song J. Experimental and statistical physics illumination of Pb(II) adsorption on magnetic chitosan-graphene oxide surface. Sep Purif Technol. 2025;354:128867.
21. Bian P, Wang M, Shao Q. Efficient adsorption of Pb^{2+} and Cd^{2+} in water by functionalized lignin-rich ragweed biochar: Combining experiments, DFT calculation, and projected density of states. Int J Biol Macromol. 2025;318:145138.
22. Ali F, Yousaf M, Sheikh NA, Khan I. Exact Solutions for the Flow of Time Fractional Model of Ternary Nanofluid: Applications in Cementitious Materials. Fractals. 2025;34(03).
23. Ouyang D, Zhuo Y, Hu L, Zeng Q, Hu Y, He Z. Research on the Adsorption Behavior of Heavy Metal Ions by Porous Material Prepared with Silicate Tailings. Minerals. 2019;9(5):291.
24. Zhou W, Deng J, Qin Z, Huang R, Wang Y, Tong S. Construction of MoS_2 nanoarrays and MoO_3 nanobelts: Two efficient adsorbents for removal of Pb(II), Au(III) and Methylene Blue. Journal of Environmental Sciences. 2022;111:38-50.
25. Abuhassan Q, Aldulaimi A, Waleed OS, PadmaPriya G, Albadr RJ, Ray S, et al. Hyaluronic acid modified iron oxide nanoparticles as a novel magnetic recyclable catalyst for one-pot preparation of pyrano[2,3-d]pyrimidines. J Organomet Chem. 2026;1052:124124.
26. Alabada R, PadmaPriya G, S S, Ray S, Rusho MA, Ibragimova S, et al. Interface-Engineered ZnO Nanorods Decorated with Clustered FeCo2S4 for Enhanced OER Electrocatalysis. J Cluster Sci. 2026;37(3).
27. Shuheil MA, Aldulaimi A, Mm R, Ray S, Waleed OS, Surya CP, et al. Construction of MWCNTs/MNPs-based copper nanocomposite as an efficient and reusable catalyst for four-component preparation of highly substituted pyridines. J Organomet Chem. 2026;1046:124011.
28. Lim JH, Moon S. A Study on Determining the Optimal Supply Level in the Early Stage of War Using Rolling- Horizon Optimization in System Dynamics. Industrial Engineering and Management Systems. 2026;25(1):71-95.
29. Mustafa KM, Oriquat GA, Nsairat H, Ibrahim HAH, Emara MH, Ibrahim AA, et al. Squilla-derived chitosan-silver/copper nanocomposites as sustainable biomaterials for targeting multidrug resistant pathogens. Microb Pathog. 2026;216:108514.
30. Hamdan AD, Al Saffar IQ. Implementation of a Modified Swarm Intelligence Algorithm in Inventory Control Practices: A Case Study. Industrial Engineering and Management Systems. 2025;24(3):354-373.
31. Li B, Li K. Efficient removal of both heavy metal ion and dyes from wastewater using magnetic response adsorbent of block polymer brush-grafted N-doped biochar. Chemosphere. 2023;340:139811.